




Data from NASA Power and surface weather stations under different climates on reference evapotranspiration estimation

Abstract – The objective of this work was to evaluate the data estimated by NASA Power in relation to that measured at surface weather stations under different climates, and to verify the effects of these data on reference evapotranspiration (ET_o) estimation. For comparison, data measured at 21 surface weather stations, located in Brazil, Israel, Australia, Portugal, and the United States of America were used, representing different Köppen climate types. The following climatic variables were analyzed daily: maximum (T_{\max}), mean (T_{mean}), and minimum (T_{\min}) air temperatures; wind speed; incident solar radiation; and mean relative humidity (RH_{mean}). Wind speed showed the highest variations and was overestimated in the Cfb, BWh, BSh, and Cfa climates. T_{mean} and mean wind speed were estimated accurately in the Csa and BWh climates, whereas T_{\max} and T_{\min} were underestimated in 13 and 9 climates, respectively; T_{\min} did not show adequate results in tropical climates. Incident solar radiation was overestimated in all climates, except in BSh, but presented the best statistical indicators among the analyzed variables. The scenarios in which ET_o was estimated using the Penman-Monteith method and data from NASA Power were consistent even for the climate type that presented the worst association between measured and estimated data.


Index terms: alternative sources, climate data, reanalysis products.

Dados da Nasa Power e de estações meteorológicas de superfície em diferentes climas na estimativa da evapotranspiração de referência

Resumo – O objetivo deste trabalho foi avaliar os dados estimados pela Nasa Power em relação aos medidos em estações meteorológicas de superfície, em diferentes climas, e verificar os efeitos destes dados na estimativa da evapotranspiração de referência (ET_o). Para comparação, foram utilizados dados medidos em 21 estações meteorológicas de superfície, localizadas no Brasil, em Israel, na Austrália, em Portugal e nos Estados Unidos da América, representando diferentes tipos climáticos de acordo com Köppen. As seguintes variáveis climáticas foram analisadas diariamente: temperaturas máxima (T_{\max}), média ($T_{\text{méd}}$) e mínima (T_{\min}) do ar; velocidade do vento; radiação solar incidente; e umidade relativa média do ar ($UR_{\text{méd}}$). A velocidade do vento apresentou as maiores variações e foi superestimada nos climas Cfb, BWh, BSh e Cfa. A $T_{\text{méd}}$ e a velocidade média do vento foram estimadas com precisão nos climas Csa e BWh, enquanto a T_{\max} e a T_{\min} foram subestimadas em 13 e 9 climas, respectivamente; a T_{\min} não apresentou resultados satisfatórios nos climas tropicais. Já a radiação solar incidente foi superestimada em todos os climas, exceto no BSh, mas apresentou os melhores indicadores estatísticos entre as variáveis analisadas. Os cenários em que a ET_o foi estimada com o método Penman-Monteith e os dados da Nasa Power foram consistentes até

Stefanie Lais Kreutz Rosa⁽¹⁾ ,
Jorge Luiz Moretti de Souza⁽¹⁾  and
Aline Aparecida dos Santos⁽¹⁾ 

⁽¹⁾ Universidade Federal do Paraná,
Departamento de Solos e Engenharia
Agrícola, Rua dos Funcionários, nº 1.540,
CEP 80035-050 Curitiba, PR, Brazil.
E-mail: skreutzrosa@gmail.com,
jmoretti@ufpr.br,
aline.santos.trabalhos@gmail.com

 Corresponding author

Received
February 03, 2023

Accepted
March 24, 2023

How to cite

ROSA, S.L.K.; SOUZA, J.L.M. de; SANTOS, A.A. dos. Data from NASA Power and surface weather stations under different climates on reference evapotranspiration estimation. *Pesquisa Agropecuária Brasileira*, v.58, e03261, 2023. DOI: <https://doi.org/10.1590/S1678-3921.pab2023.v58.03261>.

para o tipo climático que apresentou a pior associação entre dados medidos e estimados.

Termos para indexação: fontes alternativas, dados climáticos, produtos de reanálise.

Introduction

Although climate databases have improved substantially in recent decades, most countries, especially the developing ones, still suffer from shortages in meteorological data measured at surface weather stations (Aboelkhair et al., 2019). In this scenario, synthetic meteorological data provided by satellite have become a promising alternative for obtaining long and continuous data series, which can be used to compensate for insufficient measurement observations (Aboelkhair et al., 2019; Rodrigues & Braga, 2021b).

Atmospheric and sea surface observations can be used to provide long-term series of atmospheric and land surface variables through the reanalysis approach, in which numerical weather prediction models are simulated based on meteorological observations (Sheffield et al., 2006; Rodrigues & Braga, 2021b). Among the several reanalysis datasets used as sources for climate information, the National Aeronautics and Space Administration Prediction of Worldwide Energy Resources (NASA Power) has been recently highlighted. The platform provides data on several climatic variables related to solar fluxes, air temperature, relative humidity, precipitation, wind speed and direction, and soil-related parameters, such as surface and root-zone wetness and soil profile moisture (NASA, 2022). The used solar and meteorological data sets are from research carried out by NASA to support renewable energy, build energy efficiency, and meet agricultural needs, based on MERRA-2 satellite observations (GMAO, 2015).

By registering a point based on latitude and longitude coordinates in the NASA Power platform (NASA, 2022), the user is able to easily access information on any location worldwide, provided on a global grid with a spatial resolution of 1° latitude by 1° longitude for radiation datasets and 0.5° latitude by 0.625° longitude for other meteorological datasets (Stackhouse Jr., 2020). The data can be obtained on an hourly, daily, monthly, and annual time scale from 1980 to the present, being, therefore, sufficiently accurate for reliable solar and meteorological measurements

(Marzouk, 2021). This data availability facilitates and speeds up the performance of technical and scientific studies that require climatic data.

In the literature, most satellite reanalysis data are on solar radiation (Quansah et al., 2022), air temperature (Bender & Sentelhas, 2018; Aboelkhair et al., 2019), and reference evapotranspiration estimated by the Penman-Monteith method (Negm et al., 2017; Ndiaye et al., 2020). However, few studies, such as those of Rodrigues & Braga (2021b) and Monteiro et al. (2018), carried out in Portugal and Brazil, respectively, compare the performance of data from NASA Power with that of those measured at surface weather stations under different climatic conditions worldwide.

The objective of this work was to evaluate the data estimated by NASA Power in relation to that measured at surface weather stations under different climates, and to verify the effects of these data on reference evapotranspiration (ET_o) estimation.

Materials and Methods

Data from NASA Power (NASA, 2022) were compared with those from surface weather stations of Instituto Nacional de Meteorologia (INMET) in Brazil, Soil Conservation and Drainage Department (SCDD) in Israel, Bureau of Meteorology (BOM) in Australia, Instituto Português do Mar e Atmosfera (IPMA) in Portugal, and National Oceanic and Atmospheric Administration (NOAA) in the United States of America. The NASA dataset was collected on a daily scale according to the latitude and longitude of 21 locations, representative of the main climate types in Brazil, Israel, Australia, Portugal, and the United States (Table 1) according to Köppen's climate classification (Alvares et al., 2013).

The analyzed variables were: maximum (T_{\max} , °C) and minimum (T_{\min} , °C) air temperatures, wind speed (u_2 , m s⁻¹), incident solar radiation (R_s , MJ m⁻² per day), and mean relative humidity (RH_{mean} , %) recorded at INMET (2022); mean air temperature (T_{mean} , °C), u_2 , R_s , and RH_{mean} at SCDD (2022) and BOM (2022); T_{\max} and T_{\min} at IPMA (2022); and T_{\max} , T_{\min} , and u_2 at NOAA (2022). Some locations that presented RH_{mean} data (%) from NOAA were also analyzed (Table 1).

The used data were provided on a daily scale at SCDD, IPMA, and NOAA, but on an hourly scale at INMET and BOM. Therefore, the values estimated at the two latter stations were converted into daily

periodicity for the following variables: RH and u_2 , by averaging hourly values; Rs, by summing hourly values, generally recorded between 09:00 and 23:00 hours (UTC) according to the climate types; and T_{\max} and T_{\min} , by considering their magnitude over the daily period.

The period of analysis was from 1/1/2017 to 12/31/2017 for all weather stations of INMET, SCDD, IPMA, and NOAA, except for the one in the Aleknagik site, in Alaska, belonging to NOAA, for which it was from 1/1/2020 to 12/31/2020 due to the unavailability of data for previous periods. For the BOM station, the period was from 7/31/2021 to 6/21/2022. Considering the unavailability or restriction of data in the databases, the analyzed series was restricted to one year. In addition, not all climate types (i.e., Cfc, Cwc, Dfd, Dsa, Dsd, Dwa, Dw b, Dwc, Dwd, and EF) covered by Köppen's climate classification were analyzed due to data unavailability at the surface weather station or to the low quantity and quality of available data.

For the equivalent latitude and longitude of each analyzed climate, the same variables and periods were considered when using the NASA Power dataset (Table 1).

To evaluate the applicability of NASA Power data, scenarios were proposed to calculate ETo using the values of T_{\max} , T_{\min} , u_2 , Rs, and RH estimated by this database and measured at the surface weather stations. The adopted criterion were data from locations that presented the best and worst results, according to statistical indicators, for one or more of the climatic variables required by the standard Penman-Monteith method, chosen to calculate ETo (mm per day) in the present study, using the following equation presented by the American Society of Civil Engineers (Allen et al., 2005):

$$ETo = \frac{0.408 \cdot \Delta \cdot (R_n - G) + \gamma \cdot \frac{900}{(T + 273)} \cdot u_2 \cdot (e_s - e_a)}{\Delta + \gamma \cdot (1 + 0.34 \cdot u_2)}$$

Table 1. Climate type according to Köppen's classification, location and geographical coordinates of the surface weather stations, and analyzed variables.

Climate type	Location ⁽¹⁾	Latitude	Longitude	Altitude	Analyzed variable ⁽²⁾
		----- degrees -----		(m)	
Af	São Gabriel da Cachoeira-BRA	-0.12	-67.06	79.67	T_{\max} , T_{\min} , u_2 , Rs, RH
Am	São Félix do Xingu-BRA	-6.64	-51.96	211.00	T_{\max} , T_{\min} , u_2 , Rs, RH
Aw	Dianópolis-BRA	-11.59	-46.85	727.87	T_{\max} , T_{\min} , u_2 , Rs, RH
As	Surubim-BRA	-7.85	-35.75	394.00	T_{\max} , T_{\min} , u_2 , Rs, RH
BWh	Kadesh Barnea-ISR	30.90	34.39	235.00	T_{\max} , T_{\min} , u_2 , Rs, RH
BWk	Las Vegas-USA	36.21	-115.20	671.47	T_{\max} , T_{\min} , u_2
BSh	Nirim-ISR	31.33	34.39	115.00	T_{\max} , T_{\min} , u_2 , Rs, RH
BSk	Lancaster-USA	34.74	-118.21	712.62	T_{\max} , T_{\min} , u_2 , RH
Cfa	Santa Rosa-BRA	-27.89	-54.48	272.84	T_{\max} , T_{\min} , u_2 , Rs, RH
Cfb	Saint George-AUS	-28.05	148.60	198.5	T_{\max} , T_{\min} , u_2 , Rs, RH
Cfb	Caçador-BRA	-26.82	-50.99	944.26	T_{\max} , T_{\min} , u_2 , Rs, RH
Csa	Nazareth-ISR	32.69	35.33	140.00	T_{\max} , T_{\min} , u_2 , Rs, RH
Csa	Lisbon-POR	38.72	-9.15	77.00	T_{\max} , T_{\min}
Csb	Portland-USA	45.54	-122.95	62.18	T_{\max} , T_{\min} , u_2
Cwa	Araxá-BRA	-19.61	-46.95	1,018.32	T_{\max} , T_{\min} , u_2 , Rs, RH
Cwb	Diamantina-BRA	-18.23	-43.65	1,359.25	T_{\max} , T_{\min} , u_2 , Rs, RH
Dfa	Burlington-USA	40.78	-91.12	210.92	T_{\max} , T_{\min} , u_2 , RH
Dfb	Bismarck-USA	46.78	-100.76	503.22	T_{\max} , T_{\min} , u_2 , RH
Dfc	Aleknagik-USA	59.28	-158.61	24.38	T_{\max} , T_{\min}
Dsb	Spokane-USA	47.68	-117.32	595.27	T_{\max} , T_{\min} , u_2
Dsc	Anchorage-USA	61.18	-149.97	27.43	T_{\max} , T_{\min} , u_2 , RH
ET	Barrow-USA	71.28	-156.78	9.45	T_{\max} , T_{\min} , u_2 , RH

⁽¹⁾BRA, Brazil; ISR, Israel; USA, United States of America; AUS, Australia; and POR, Portugal. Weather stations of: Instituto Nacional de Meteorologia in Brazil, Soil Conservation and Drainage Department in Israel, National Oceanic and Atmospheric Administration station in the United States, Bureau of Meteorology in Australia, and Instituto Português do Mar e Atmosfera in Portugal. ⁽²⁾ T_{\max} , maximum air temperature; T_{\min} , minimum air temperature; T_{mean} , mean air temperature; u_2 , wind speed; Rs, incident solar radiation; and RH, mean relative humidity.

where Δ is the slope vapor pressure curve ($\text{kPa } ^\circ\text{C}^{-1}$); R_n is the net radiation at crop surface (MJ m^{-2} per day); G is the soil heat flux density (MJ m^{-2} per day); γ is the psychrometric constant ($\text{kPa } ^\circ\text{C}^{-1}$); T is the mean daily air temperature at a 2.0 m height ($^\circ\text{C}$); u_2 is the wind speed at a 2.0 m height (m s^{-1}); e_s is the saturation vapor pressure (kPa); and e_a is the actual vapor pressure (kPa).

The e_a was calculated using the RH_{mean} due to the unavailability of RH_{max} and RH_{min} data in the databases as recommended by Paredes & Pereira (2019). For this, the following equation of Allen et al. (2005) was used:

$$e_a = \frac{RH_{\text{mean}}}{\frac{50}{e_s(T_{c_{\text{min}}})} + \frac{50}{e_s(T_{c_{\text{max}}})}}$$

where $e_s(T_{c_{\text{min}}})$ and $e_s(T_{c_{\text{max}}})$ are the saturation pressure (kPa) calculated as a function of the minimum and maximum air temperatures, respectively; and RH_{mean} is the mean relative humidity of the air observed on the day (%).

NASA Power data in relation to those measured at the surface weather stations and the ETo estimated with the reanalyzed climatic data were evaluated based on linear regression analyses and the following statistical indicators: mean absolute error (MAE), root mean square error (RMSE), index of agreement (d), Pearson's correlation coefficient (r), and the Nash-Sutcliffe coefficient (Nash & Sutcliffe, 1970). The analyses were performed using the hydroGOF package of the RStudio software (Zambrano-Bigiarini, 2020).

Results and Discussion

The highest discrepancies between data from NASA Power and the surface stations were found for u_2 , which presented an expressive overestimation mainly in the Cfb climate (Table 2). Apparently, the u_2 values were recorded incorrectly at the INMET station under this climate during the experimental period, since they differed significantly from those found by Santos et al. (2021) when evaluating the average seasonal trend of the climatic variables of ten surface stations in Cfb climate regions in the state of Paraná, Brazil.

In relation to NASA Power data, the u_2 variable was also overestimated in the As, BWh, BSh, Cfa (only

at the INMET station), Cwa, and Cwb climates, but underestimated in the Af, Am, Aw, BWk, BSk, Cfa (only at the BOM station), Csa, Csb, Dfa, Dfb, Dsb, Dsc, and ET climates. The lowest underestimation was observed in the Am climate, in which the mean value of u_2 estimated by satellite was lower than that measured at the surface weather station. Using the alternative Moretti-Jerszurki-Silva method to estimate ETo in different Brazilian climatic zones from 2004 to 2014, Jerszurki et al. (2017) found an annual u_2 mean of 1.98 m s^{-1} for the Am climate, close to the measured value analyzed in the present study. The highest similarities between measured and estimated u_2 values occurred in the Aw, Cwb, Cwa, and BSh climates. Specifically in BSh, the u_2 value was 2.17 m s^{-1} , similar to that of 2.28 m s^{-1} reported by Jerszurki et al. (2017). When u_2 values are inconsistent and cause doubts as to their accuracy, ETo should be estimated using alternative methods, such as that of Hargreaves-Samani, which do not consider u_2 as an input in the equation and, at the same time, present results equivalent to those obtained with the Penman-Monteith method.

The T_{mean} in the BWh, BSh, Cfa, and Csa climates showed the smallest deviation in relation to the measured data (Table 2). This variable was underestimated in 0.05% in Csa and overestimated in 1.46% in BWh, indicating that the observed differences were insignificant and did not affect the accuracy of the NASA Power dataset regarding temperature in these sites. Similar results were found by Aboelkhair et al. (2019) for T_{mean} when evaluating T_{max} , T_{min} , T_{mean} , dew point temperature, and RH data from 20 surface weather stations in Egypt, on a monthly scale, in the period from 1983 to 2006, predominantly in the BWh climate. Likewise, Marzouk (2021), analyzing T_{mean} , RH, atmospheric pressure, and daily precipitation data from NASA Power, also in the BWh climate, observed that T_{mean} showed a better agreement between the analyzed variables, indicating the reliability of the data set for this variable.

In relation to NASA Power data, R_s was overestimated in all sites, except in the As and BSh climates, showing the highest discrepancy of 109.33% under the Cfa climate in Saint George, Australia. Apparently, the data records at this weather station presented some error since the R_s measured for the same climate at the INMET station was 17.09 MJ m^{-2} per day, similar to that of 17.01 MJ m^{-2} per day

reported by Jerszurki et al. (2017), also using INMET data collected under the Cfa climate in Brazil.

According to the used statistical indicators (Table 3), the best fits between estimated and measured data occurred for T_{\max} in the Dfa, Dfb, Dfc, Dsb, and Dsc continental climates. This variable also showed good fits in the ET polar climate and was suitable for the BWk and BSk semi-arid climates. The BWk and BSh climates are located, respectively, in Kadesh Barnea and Nirim, Israel, within the latitude and longitude limits of 30° north latitude (area predominantly influenced by the Mediterranean Sea)

and 30° west longitude. In these latitude and longitude conditions, Aboelkhair et al. (2019) found that NASA Power accurately simulates T_{\max} , as observed in the present study (Table 1).

Good fits were also found for T_{\min} in continental and polar climates. Furthermore, this variable also showed good statistical indicators in the BWk and BSk semi-arid climates and the Cfa (at INMET), Cfb, Csa, Csb, Cwa, and Cwb humid subtropical climates. However, T_{\min} did not present satisfactory results in the Af, Am, and Aw tropical climates (Table 3).

Table 2. Annual averages of estimated (E) and observed (O) climatic variables⁽¹⁾, with respective percentage of over-⁽⁺⁾ and underestimation⁽⁻⁾.

Climate type ⁽²⁾	RH _{mean} (%)			u ₂ (m s ⁻¹)			T _{max} (°C)			T _{mean} (°C)			T _{min} (°C)			Rs (MJ m ⁻² per day)		
	O	E	(%)	O	E	(%)	O	E	(%)	O	E	(%)	O	E	(%)	O	E	(%)
Af	85.67	91.72	7.07 ⁽⁺⁾	0.59	0.16	270.0 ⁽⁻⁾	31.28	28.50	9.77 ⁽⁻⁾	—	—	—	23.06	23.40	1.46 ⁽⁺⁾	15.09	16.72	10.81 ⁽⁺⁾
Am	78.50	75.35	4.19 ⁽⁻⁾	1.26	0.13	864.7 ⁽⁻⁾	32.65	31.28	4.37 ⁽⁻⁾	—	—	—	21.97	22.33	1.68 ⁽⁺⁾	17.85	18.42	3.20 ⁽⁺⁾
As	72.41	77.88	7.55 ⁽⁺⁾	1.56	3.46	121.0 ⁽⁺⁾	30.50	30.13	1.23 ⁽⁻⁾	—	—	—	20.58	20.48	0.82 ⁽⁻⁾	20.01	19.53	2.48 ⁽⁻⁾
Aw	58.48	56.01	4.42 ⁽⁻⁾	2.27	2.25	0.8 ⁽⁻⁾	30.84	32.84	6.46 ⁽⁺⁾	—	—	—	20.40	21.39	4.86 ⁽⁺⁾	20.13	20.64	2.56 ⁽⁺⁾
BWh	59.63	62.78	5.28 ⁽⁺⁾	1.74	2.35	34.7 ⁽⁺⁾	—	—	—	19.69	19.97	1.46 ⁽⁺⁾	—	—	—	20.06	21.62	7.73 ⁽⁺⁾
BWk	—	—	—	8.05	2.68	200.7 ⁽⁻⁾	27.60	27.96	1.33 ⁽⁺⁾	—	—	—	15.47	13.92	11.10 ⁽⁻⁾	—	—	—
BSh	72.65	67.79	7.17 ⁽⁻⁾	2.17	2.52	16.2 ⁽⁺⁾	—	—	—	19.95	21.29	6.71 ⁽⁺⁾	—	—	—	20.43	19.72	3.60 ⁽⁻⁾
BSk	40.87	47.00	14.98 ⁽⁺⁾	11.08	2.23	395.9 ⁽⁻⁾	26.08	25.81	1.06 ⁽⁻⁾	—	—	—	9.42	10.86	15.22 ⁽⁺⁾	—	—	—
Cfa ¹	55.38	58.66	5.92 ⁽⁺⁾	4.70	2.93	60.2 ⁽⁻⁾	—	—	—	21.55	20.92	3.04 ⁽⁻⁾	—	—	—	9.65	20.20	109.3 ⁽⁺⁾
Cfa ²	74.04	83.02	12.13 ⁽⁺⁾	1.30	2.00	53.9 ⁽⁺⁾	27.27	25.49	6.96 ⁽⁻⁾	—	—	—	15.38	14.46	6.33 ⁽⁻⁾	17.09	17.33	1.40 ⁽⁺⁾
Cfb	77.27	83.84	8.50 ⁽⁺⁾	0.13	1.55	1109.8 ⁽⁺⁾	23.62	22.97	2.83 ⁽⁻⁾	—	—	—	12.39	12.26	1.02 ⁽⁻⁾	13.03	15.47	18.76 ⁽⁺⁾
Csa ¹	57.21	57.63	0.73 ⁽⁺⁾	1.70	0.93	82.6 ⁽⁻⁾	—	—	—	20.70	20.69	0.05 ⁽⁻⁾	—	—	—	18.23	20.03	9.86 ⁽⁺⁾
Csa ²	—	—	—	—	—	—	22.37	19.20	16.49 ⁽⁻⁾	—	—	—	14.10	14.57	3.30 ⁽⁺⁾	—	—	—
Csb	—	—	—	5.06	0.61	730.3 ⁽⁻⁾	17.10	14.49	18.03 ⁽⁻⁾	—	—	—	5.71	5.62	1.53 ⁽⁻⁾	—	—	—
Cwa	62.36	68.10	9.19 ⁽⁺⁾	2.07	2.30	11.3 ⁽⁺⁾	27.72	27.83	0.41 ⁽⁺⁾	—	—	—	17.08	15.99	6.79 ⁽⁻⁾	18.88	19.23	1.88 ⁽⁺⁾
Cwb	73.51	67.39	9.08 ⁽⁻⁾	2.51	2.74	9.6 ⁽⁺⁾	23.71	27.72	16.93 ⁽⁺⁾	—	—	—	14.44	15.47	7.14 ⁽⁺⁾	18.17	18.34	0.92 ⁽⁺⁾
Dfa	71.45	70.26	1.68 ⁽⁻⁾	8.63	3.28	163.0 ⁽⁻⁾	17.20	17.46	1.51 ⁽⁺⁾	—	—	—	6.86	6.60	4.07 ⁽⁻⁾	—	—	—
Dfb	65.43	65.07	0.55 ⁽⁻⁾	9.04	3.59	151.5 ⁽⁻⁾	13.65	12.80	6.65 ⁽⁻⁾	—	—	—	0.42	1.37	222.44 ⁽⁺⁾	—	—	—
Dfc	—	—	—	—	—	—	5.44	2.81	93.38 ⁽⁻⁾	—	—	—	-2.48	-4.16	40.34 ⁽⁻⁾	—	—	—
Dsb	—	—	—	4.33	1.97	120.0 ⁽⁻⁾	15.35	13.23	15.99 ⁽⁻⁾	—	—	—	4.09	2.66	53.73 ⁽⁻⁾	—	—	—
Dsc	75.57	86.05	13.86 ⁽⁺⁾	5.10	1.76	189.5 ⁽⁻⁾	6.27	3.97	57.82 ⁽⁻⁾	—	—	—	-0.55	-0.94	41.21 ⁽⁻⁾	—	—	—
ET	83.61	93.26	11.54 ⁽⁺⁾	13.46	5.37	150.7 ⁽⁻⁾	-4.86	-5.55	12.51 ⁽⁻⁾	—	—	—	-10.35	-8.18	20.97 ⁽⁺⁾	—	—	—

⁽¹⁾RH_{mean}, mean relative humidity; u₂, wind speed; T_{max}, maximum air temperature; T_{mean}, mean air temperature; T_{min}, minimum air temperature; and Rs, incident solar radiation. ⁽²⁾Cfa¹, Cfa², Csa¹, and Csa² in the weather stations of Bureau of Meteorology in Australia, Instituto Nacional de Meteorologia in Brazil, Soil Conservation and Drainage Department in Israel, and Instituto Português do Mar e Atmosfera in Portugal, respectively.

Table 3. Statistical indicators of associations between the estimated and observed Köppen climate type variables.

Indicator ⁽¹⁾	Climate type ⁽²⁾																			
	Af	Am	Aw	As	BWh	BWk	BSh	BSk	Cfa ¹	Cfa ²	Cfb	Csa ¹	Csa ²	Csb	Cwa	Cwb	Dfa	Dfb	Dfc	Dsb
Mean relative humidity (%)																				
MAE	6.10	9.74	5.03	5.85	5.80	—	7.10	9.14	6.19	9.45	6.96	5.22	—	—	7.00	7.81	8.44	8.36	—	—
RMSE	6.84	12.78	6.55	6.88	8.05	—	8.99	11.23	7.61	12.14	8.34	6.98	—	—	8.91	9.18	10.18	10.72	—	—
NSE	-5.52	0.59	0.90	0.35	0.48	—	-0.77	0.74	0.71	-2.03	-0.99	0.72	—	—	0.69	0.40	0.14	0.60	—	—
d	0.44	0.81	0.97	0.84	0.86	—	0.75	0.92	0.93	0.65	0.72	0.92	—	—	0.92	0.84	0.79	0.85	—	—
R ²	0.27	0.76	0.91	0.77	0.61	—	0.54	0.83	0.79	0.52	0.63	0.73	—	—	0.82	0.68	0.42	0.60	—	—
r	0.52	0.87	0.96	0.87	0.78	—	0.73	0.91	0.89	0.72	0.80	0.85	—	—	0.90	0.83	0.65	0.77	—	—
Wind speed (m s ⁻¹)																				
MAE	0.43	1.13	0.38	2.19	0.63	5.37	0.47	8.83	1.68	0.7	1.43	0.77	—	4.45	0.41	0.46	5.34	5.46	—	2.52
RMSE	0.45	1.16	0.49	2.41	0.75	6.18	0.60	10.41	1.81	0.8	1.47	0.87	—	5.31	0.52	0.58	5.76	6.13	—	3.20
NSE	-61.63	-415.7	0.79	-17.27	-0.31	-19.35	0.22	-157.2	-2.58	-0.91	-9.18	-13.63	—	-615.2	0.6	0.66	-17.45	-18.32	—	-15.45
d	0.16	0.07	0.93	0.33	0.68	0.38	0.78	0.13	0.64	0.59	0.33	0.35	—	0.09	0.87	0.91	0.39	0.40	—	0.43
R ²	0.04	0.04	0.8	0.12	0.55	0.64	0.5	0.21	0.83	0.57	0.49	0.27	—	0.56	0.68	0.73	0.86	0.83	—	0.62
r	-0.21	-0.19	0.89	0.34	0.74	0.8	0.71	0.46	0.91	0.75	0.70	0.52	—	0.75	0.83	0.86	0.93	0.91	—	0.79
Maximum temperature (°C)																				
MAE	2.91	2.59	2.48	1.19	—	0.97	—	1.56	—	2.27	1.82	—	3.65	2.83	1.72	4.1	1.58	1.86	2.85	2.22
RMSE	3.27	3.09	2.84	1.50	—	1.27	—	2.04	—	2.66	2.24	—	4.63	3.18	2.08	4.54	1.98	2.48	3.43	2.51
NSE	-8.7	0.46	0.24	0.78	—	0.98	—	0.95	—	0.63	0.62	—	-0.71	0.86	0.39	-1.45	0.97	0.97	0.92	0.95
d	0.41	0.80	0.78	0.94	—	1.00	—	0.99	—	0.92	0.92	—	0.78	0.97	0.84	0.64	0.99	0.99	0.98	0.99
R ²	0.30	0.58	0.62	0.79	—	0.98	—	0.95	—	0.84	0.76	—	0.77	0.97	0.51	0.59	0.97	0.97	0.97	0.99
r	0.55	0.76	0.79	0.89	—	0.99	—	0.98	—	0.92	0.87	—	0.88	0.99	0.71	0.77	0.99	0.99	0.99	0.98
Mean temperature (°C)																				
MAE	—	—	—	—	0.71	—	1.44	—	0.77	—	—	0.98	—	—	—	—	—	—	—	—
RMSE	—	—	—	—	0.97	—	1.70	—	1.02	—	—	1.25	—	—	—	—	—	—	—	—
NSE	—	—	—	—	0.98	—	0.89	—	0.97	—	—	0.97	—	—	—	—	—	—	—	—
d	—	—	—	—	0.99	—	0.97	—	0.99	—	—	0.99	—	—	—	—	—	—	—	—
R ²	—	—	—	—	0.98	—	0.97	—	0.97	—	—	0.98	—	—	—	—	—	—	—	—
r	—	—	—	—	0.99	—	0.99	—	0.99	—	—	0.99	—	—	—	—	—	—	—	—
Minimum temperature (°C)																				
MAE	0.74	1.06	1.28	0.57	—	2.27	—	3.90	—	1.54	1.46	—	1.57	1.53	1.41	1.23	1.36	2.20	2.78	2.16
RMSE	0.93	1.44	1.61	0.70	—	2.70	—	5.08	—	1.95	1.78	—	2.12	1.89	1.73	1.46	1.71	2.84	3.63	2.75
NSE	-0.61	0.33	0.21	0.75	—	0.90	—	0.35	—	0.84	0.83	—	0.45	0.86	0.65	0.66	0.97	0.94	0.91	0.91
d	0.53	0.80	0.80	0.95	—	0.97	—	0.87	—	0.96	0.96	—	0.91	0.97	0.9	0.92	0.99	0.98	0.97	0.97
R ²	0.07	0.45	0.57	0.83	—	0.93	—	0.67	—	0.88	0.85	—	0.83	0.89	0.79	0.84	0.97	0.95	0.93	0.94
r	0.26	0.67	0.75	0.91	—	0.97	—	0.82	—	0.94	0.92	—	0.91	0.94	0.89	0.92	0.99	0.97	0.96	0.97
Incident solar radiation (MJ m ⁻² per day)																				
MAE	2.47	1.8	1.45	2.21	1.67	—	1.14	—	11.18	1.15	2.80	1.88	—	—	1.48	1.84	—	—	—	—
RMSE	3.04	2.22	2.09	2.82	1.96	—	1.67	—	12.04	1.53	3.39	2.09	—	—	1.99	2.34	—	—	—	—
NSE	0.44	0.64	0.72	0.09	0.92	—	0.94	—	-1.78	0.96	0.73	0.92	—	—	0.83	0.81	—	—	—	—
d	0.88	0.91	0.94	0.84	0.98	—	0.99	—	0.58	0.99	0.93	0.98	—	—	0.96	0.96	—	—	—	—
R ²	0.70	0.72	0.79	0.62	0.97	—	0.95	—	0.62	0.97	0.87	0.98	—	—	0.85	0.85	—	—	—	—
r	0.83	0.85	0.89	0.79	0.98	—	0.98	—	0.79	0.98	0.93	0.99	—	—	0.92	0.92	—	—	—	—

⁽¹⁾MAE, mean absolute error; RMSE, root mean square error; NSE, Nash-Sutcliffe coefficient; d, index of agreement; R², coefficient of determination; and r, Pearson's correlation coefficient. ⁽²⁾Cfa¹, Cfa², Csa¹, and Csa² in the weather stations of Bureau of Meteorology in Australia, Instituto Nacional de Meteorologia in Brazil, Soil Conservation and Drainage Department in Israel, and Instituto Português do Mar e Atmosfera in Portugal, respectively.

Regarding the accuracy of NASA Power in estimating variables related to air temperature, White et al. (2008) found that the data series provided reliable daily T_{\max} and T_{\min} data for the United States from 1983 to 2004, considering 855 NOAA stations. The authors observed a RMSE of 4.1°C and 3.7°C for T_{\max} and T_{\min} , respectively, and a $R^2 = 0.88$ for both. The T_{mean} estimated by NASA Power was satisfactory in all locations with the BWh, BSh, Cfa, and Csa climates, showing a low MAE and RMSE, with a high NSE and high d- and r-values.

Despite the good statistical indicators obtained for T_{\max} and T_{\min} in continental and polar climates, NASA Power did not accurately estimate RH_{mean} and u_2 under these conditions. The RH_{mean} presented $r < 0.77$ in the Dfa, Dfb, and Dsc climates, and $r = -0.12$ in the ET climate. Despite the $r > 0.78$ in Dfa, Dfb, and Dsc and $r = 0.94$ for u_2 in ET, the linear associations resulted in a negative NSE, an indicative of the low adjustment of the estimated data. However, the RH_{mean} estimated by NASA Power showed better fits for the Aw tropical climate. In addition, the best indicators were observed in the BSk semi-arid and Cwa humid subtropical climates. In the present study, the RH_{mean} obtained for the BSh climate showed a RMSE = 8.99%, which was much lower than that of up to 31.75% reported by Aboelkhair et al. (2019) for the BWh semi-arid climate. These findings indicate that NASA Power showed a higher accuracy in estimating RH_{mean} in warmer climates (tropical, subtropical, and semi-arid), but requires adjustments to be used in colder climates (continental and polar).

The u_2 variable presented a negative NSE in almost all climates. Good indicators were observed only in the Aw, Cwa, and Cwb climates, with $r \geq 0.83$. Despite the low MAE and RMSE values for u_2 in the Csa climate, NSE was negative and the d and r statistical indicators were low, indicating the poor performance of NASA Power to estimate u_2 under these conditions. Likewise, Rodrigues & Braga (2021a), evaluating daily T_{\max} , T_{\min} , Rs, RH, and u_2 estimated by NASA Power and measured at 14 surface weather stations in the Csa climate, in the Alentejo region in Southern Portugal, found a good alignment between the different databases, except for u_2 . Therefore, although NASA Power accurately estimates many of the analyzed climate variables, u_2 still needs to be better managed and evaluated.

Among the analyzed variables, Rs showed the best statistical indicators overall. The worst values occurred in the Cfa climate in Saint George, Australia. Therefore, there probably was an error in the Rs data records at the BOM station, since the values measured for this variable in same climate type at the INMET station were similar to those provided by NASA (Table 2). In all other climates, Rs showed good indicators, with $1.14 \text{ MJ m}^{-2} \text{ per day} \leq \text{RMSE} \leq 3.39 \text{ MJ m}^{-2} \text{ per day}$ and $0.88 \leq d \leq 0.99$. The results found for Rs were very close to those obtained by Monteiro et al. (2018), on a daily scale, who found RMSE = 3.10 MJ m⁻² per day and d = 0.99 when comparing the INMET and NASA Power databases in Brazil. According to these authors, the high d indicates the precision of NASA Power to estimate Rs.

Overall, the reanalysis data estimated with the NASA Power database follow a trend very similar to that of the data measured at the INMET, SCDD, BOM, IPMA, and NOAA surface weather stations. The exceptions were variables u_2 in almost all climates (except Aw, Cwa, and Cwb), T_{\max} and T_{\min} in tropical climates, and RH_{mean} in continental and polar climates. The statistical indicators also resulted in a good association for most variables and climates, showing reliability and robustness to be used in data analysis procedures. Similarly, Monteiro et al. (2018) concluded that NASA Power products can be used as a reasonably accurate source of climatic data for agricultural activities at regional and national spatial scales. However, attention is necessary mainly concerning variables u_2 , T_{\max} , and T_{\min} in tropical climates and RH_{mean} in continental and polar climates, which showed a higher discrepancy in relation to the values measured at the surface stations. For the other variables in different locations, the data from NASA Power can be considered for application in areas of agricultural sciences, especially for water and soil engineering.

The ETo estimated using T_{\max} , T_{\min} , u_2 , Rs, and RH_{mean} data from the surface weather stations and the NASA Power database was calculated for the worst statistical indicator (Table 3), observed in the Af climate in São Gabriel da Cachoeira, Brazil, where all analyzed climatic variables performed poorly, except Rs. The best indicators were obtained for T_{\max} and T_{\min} in the Cfa climate (INMET) and for u_2 and RH_{mean} in the Aw climate in Dianópolis, Brazil, which presented at least two variables with the best indexes. However,

Cfa (at INMET) showed a negative NSE for u_2 , which explains why Aw was considered in ETo estimation. Therefore, ETo was calculated under two climates in Brazil: Af in the state of Amazonas (at a latitude of -0.1252, longitude of -67.0612, and altitude of 79.67 m) and Aw in the state of Tocantins (at a latitude of -11.5944, longitude of -46.8472, and altitude of 727.87) in the period from 1/1/2017 to 12/31/2017, representing the worst and best statistical indicators, respectively (Figure 1).

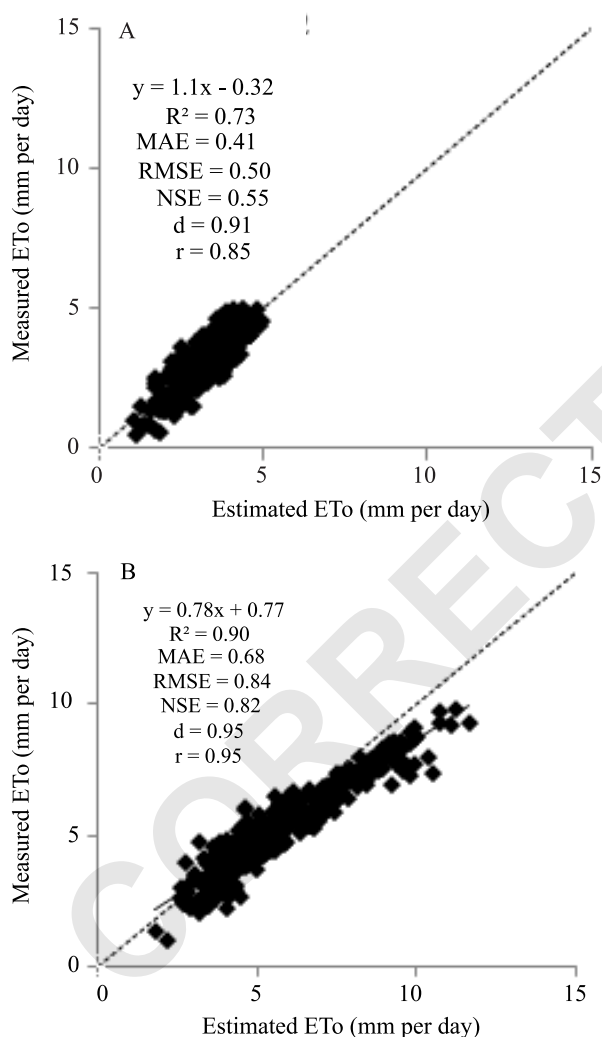


Figure 1. Linear regression analysis associating reference evapotranspiration (ETo) calculated with estimated and measured data for the locations under the Aw and Af climates that showed the best (A) and worst (B) adjustments, respectively, according to the used statistical indicators.

The association of the ETo calculated with measured vs. estimated data indicated satisfactory adjustments, even for the worst condition in the Af climate. In the better condition in the Aw climate, the association indicated $r = 0.90$ (Figure 1 B). The average values of ETo, calculated with measured and estimated climatic data, were 3.26 and 3.37 mm per day in the Af climate and 5.34 and 5.82 mm per day in the Aw climate, respectively. The highest MAE and RMSE values observed in Aw are associated with the highest ETo values that generally occur under this climate (Jerszurki et al., 2017).

The average values of the ETo calculated for the Af and Aw climates agree with those obtained by Oliveira (2018), based on Allen et al. (2005), using data from 22 and 65 stations under the Af and Aw climates, respectively. Jerszurki et al. (2017) also observed a higher ETo value of 4.09 mm per day in the Aw climate, compared with that of 3.73 mm per day in Af in Brazil.

Considering the good statistical indicators obtained even for the worst location in the Af climate, ETo was also calculated for the climates in Table 1 that had the input variables (T_{max} , T_{min} and/or T_{mean} , u_2 , R_s , and RH_{mean}) required by the Allen et al. (2005) method. The over- and underestimates obtained in the analyzes did not significantly affect the ETo estimate (Table 2), as verified in the associations shown in Figure 2. Even with the inconsistencies in u_2 and R_s in the Cfb and Cfa (at BOM) climates, respectively, the associations of the daily ETo obtained with estimated and measured data for different Köppen climate types resulted in good fits (Figure 2 E and G).

The present study showed promising ETo results (Figure 2), as well as the easy use of the NASA Power database to extract data without requiring knowledge of geographic information system software or satellite image processing (Marzouk, 2021). However, since ETo is used to estimate crop evapotranspiration ($ET_c = ETo \times kc$) and underestimates can accumulate under field conditions, it is difficult to manage and account for water balance for irrigated crops. As a result, the achieved yields may be lower due to the reduced water availability for the plant cycle. However, this can only be better elucidated in studies more applied to water and soil engineering in irrigated crops.

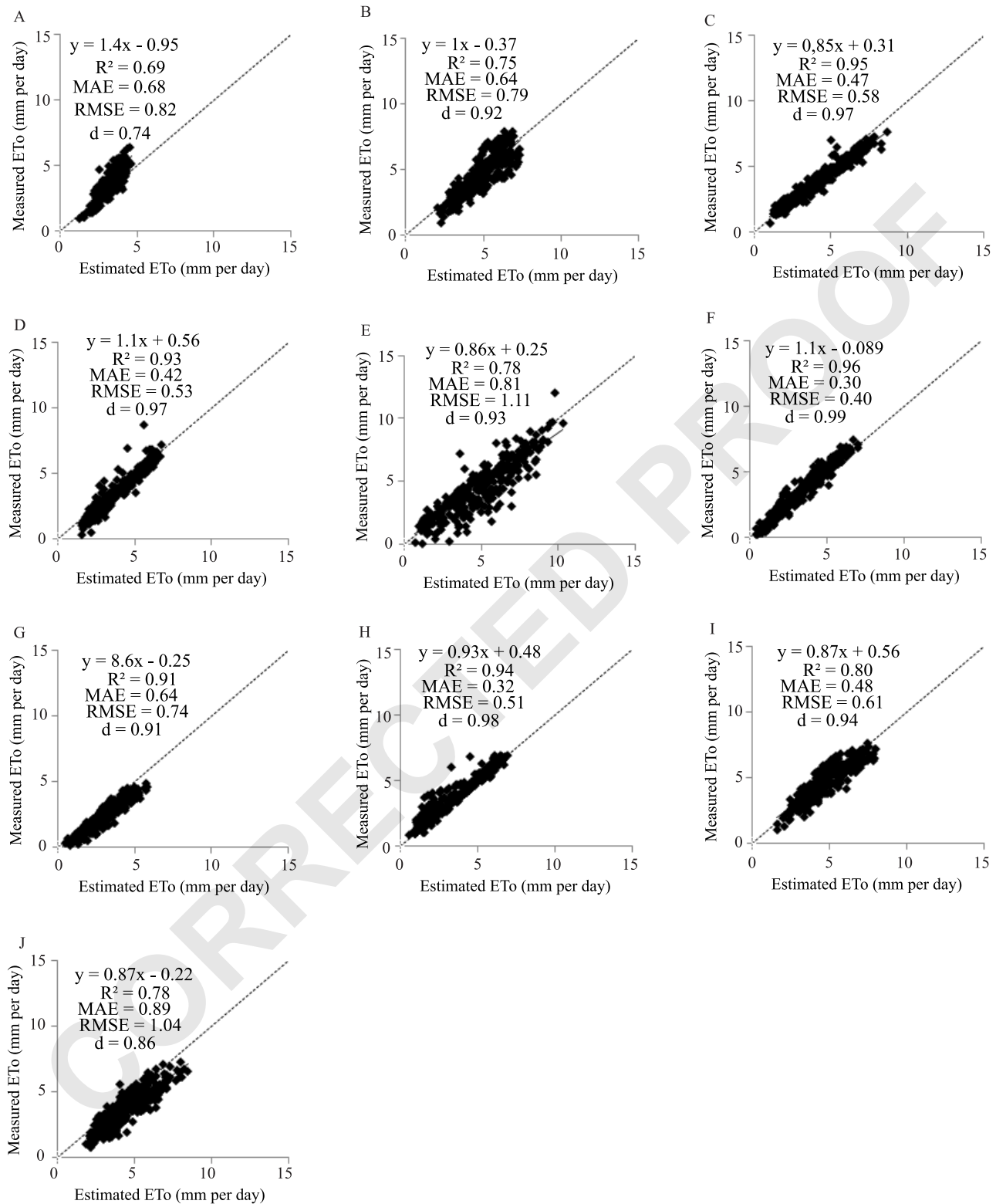


Figure 2. Daily reference evapotranspiration (ETo) obtained with estimated vs. measured data for the following Köppen climate types: Am (A), As (B), BWh (C), BSh (D), Cfa at the Bureau of Meteorology station in Australia (E), Cfa at the Instituto Nacional de Meteorologia station in Brazil (F), Cfb (G), Csa (H), Cwa (I), and Cwb (J).

Conclusions

1. NASA Power estimates for air temperature are consistent with the data measured at surface weather stations in continental, polar, and semi-arid climates, but not in tropical ones.

2. In the analyzed climate types, the NASA Power database accurately estimates maximum, minimum, and mean temperatures, as well as incident solar radiation, but shows the highest deviations for wind speed in relation to the data measured at surface stations and a more accurate mean relative humidity in warmer climates.

3. NASA Power data are accurate to estimate reference evapotranspiration with the Penman-Monteith method.

Acknowledgments

To Coordenação de Aperfeiçoamento de Pessoal de Nível Superior (CAPES), for financing, in part, this study (Finance Code 001).

References

- ABOELKHAIR, H.; MORSY, M.; EL AFANDI, G. Assessment of agroclimatology NASA POWER reanalysis datasets for temperature types and relative humidity at 2 m against ground observations over Egypt. **Advances in Space Research**, v.64, p.129-142, 2019. DOI: <https://doi.org/10.1016/j.asr.2019.03.032>.
- ALLEN, R.G.; WALTER, I.A.; ELLIOTT, R.; HOWELL, T.; ITENFISU, D.; JENSEN, M. (Ed.). **The ASCE standardized reference evapotranspiration equation**. Reston: American Society of Civil Engineers, 2005. DOI: <https://doi.org/10.1061/9780784408056>.
- ALVARES, C.A.; STAPE, J.L.; SENTELHAS, P.C.; GONÇALVES, J.L. de M.; SPAROVEK, G. Köppen's climate classification map for Brazil. **Meteorologische Zeitschrift**, v.22, p.711-728, 2013. DOI: <https://doi.org/10.1127/0941-2948/2013/0507>.
- BENDER, F.D.; SENTELHAS, P.C. Solar radiation models and gridded databases to fill gaps in weather series and to project climate change in Brazil. **Advances in Meteorology**, v.2018, art.6204382, 2018. DOI: <https://doi.org/10.1155/2018/6204382>.
- BOM. **Bureau of Meteorology**. Available at: <http://www.bom.gov.au/>. Accessed on: Aug. 22 2022.
- GMAO. Global Modeling and Assimilation Office. **MERRA-2 tavgM_2d_flx_Nx**: 2d, Monthly mean, Time-Averaged, Single-Level, Assimilation, Surface Flux Diagnostics V5.12.4. Greenbelt: Goddard Earth Sciences Data and Information Services Center, 2015. DOI: <https://doi.org/10.5067/0JRLVL8YV2Y4>.
- INMET. **Instituto Nacional de Meteorologia**. Available at: <https://portal.inmet.gov.br/>. Accessed on: Aug. 22 2022.
- IPMA. Instituto Português do Mar e da Atmosfera. **Long data series**. Available at: <https://www.ipma.pt/en/oclima/series/longas/>. Accessed on: Aug. 22 2022.
- JERSZURKI, D.; SOUZA, J.L.M.; SILVA, L.C.R. Expanding the geography of evapotranspiration: an improved method to quantify land-to-air water fluxes in tropical and subtropical regions. **PLoS ONE**, v.12, e0180055, 2017. DOI: <https://doi.org/10.1371/journal.pone.0180055>.
- MARZOUK, O.A. Assessment of global warming in Al Buraimi, sultanate of Oman based on statistical analysis of NASA POWER data over 39 years, and testing the reliability of NASA POWER against meteorological measurements. **Helyon**, v.7, e06625, 2021. DOI: <https://doi.org/10.1016/j.heliyon.2021.e06625>.
- MONTEIRO, L.A.; SENTELHAS, P.C.; PEDRA, G.U. Assessment of NASA/POWER satellite-based weather system for Brazilian conditions and its impact on sugarcane yield simulation. **International Journal of Climatology**, v.38, p.1571-1581, 2018. DOI: <https://doi.org/10.1002/joc.5282>.
- NASA. National Aeronautics and Space Administration. **Power Data Access Viewer**: Prediction of Worldwide Energy Resource. Available at: <https://power.larc.nasa.gov/data-access-viewer/>. Accessed on: Mar. 22 2022.
- NASH, J.E.; SUTCLIFFE, J.V. River flow forecasting through conceptual models: part I – a discussion of principles. **Journal of Hydrology**, v.10, p.282-290, 1970. DOI: [https://doi.org/10.1016/0022-1694\(70\)90255-6](https://doi.org/10.1016/0022-1694(70)90255-6).
- NDIAYE, P.M.; BODIAN, A.; DIOP, L.; DEME, A.; DEZETTER, A.; DJAMAN, K.; OGILVIE, A. Trend and sensitivity analysis of reference evapotranspiration in the Senegal river basin using NASA meteorological data. **Water**, v.12, art.1957, 2020. DOI: <https://doi.org/10.3390/w12071957>.
- NEGM, A.; JABRO, J.; PROVENZANO, G. Assessing the suitability of American National Aeronautics and Space Administration (NASA) agro-climatology archive to predict daily meteorological variables and reference evapotranspiration in Sicily, Italy. **Agricultural and Forest Meteorology**, v.244/245, p.111-121, 2017. DOI: <https://doi.org/10.1016/j.agrformet.2017.05.022>.
- NOAA. National Oceanic and Atmospheric Administration. **Climate Data Online**. Available at: <https://www.ncdc.noaa.gov/cdo-web/>. Accessed on: Mar. 30 2022.
- OLIVEIRA, S.R. **Ajuste do método Moretti-Jerszurki-Silva para estimar a evapotranspiração de referência diária e horária dos tipos climáticos brasileiros**. 2018. 537p. Tese (Doutorado) – Universidade Federal do Paraná, Curitiba.
- PAREDES, P.; PEREIRA, L.S. Computing FAO56 reference grass evapotranspiration PM-ET₀ from temperature with focus on solar radiation. **Agricultural Water Management**, v.215, p.86-102, 2019. DOI: <https://doi.org/10.1016/j.agwat.2018.12.014>.
- QUANSAH, A.D.; DOGBEY, F.; ASILEVI, P.J.; BOAKYE, P.; DARKWAH, L.; ODURO-KWARTENG, S.; SOKAMA-NEUYAM, Y.; MENSAH, P. Assessment of solar radiation

resource from the NASA-POWER reanalysis products for tropical climates in Ghana towards clean energy application. **Scientific Report**, v.12, art.10684, 2022. DOI: <https://doi.org/10.1038/s41598-022-14126-9>.

RODRIGUES, G.C.; BRAGA, R.P. Estimation of daily reference evapotranspiration from NASA POWER reanalysis products in a hot summer Mediterranean climate. **Agronomy**, v.11, art.2077, 2021a. DOI: <https://doi.org/10.3390/agronomy11102077>.

RODRIGUES, G.C.; BRAGA, R.P. Evaluation of NASA POWER reanalysis products to estimate daily weather variables in a hot summer Mediterranean climate. **Agronomy**, v.11, art.1207, 2021b. DOI: <https://doi.org/10.3390/agronomy11061207>.

SANTOS, A.A. dos; SOUZA, J.L.M. de; ROSA, S.L.K. Hourly and daily reference evapotranspiration with ASCE-PM model for Paraná State, Brazil. **Revista Brasileira de Meteorologia**, v.36, p.197-209, 2021. DOI: <https://doi.org/10.1590/0102-77863610009>.

SCDD. **Soil Conservation and Drainage Department**. Available at: <https://meteo.co.il/report/SingleStationReport>. Accessed on: Aug. 22 2022.

SHEFFIELD, J.; GOTETI, G.; WOOD, E.F. Development of a 50-year high-resolution global dataset of meteorological forcings for land surface modeling. **Journal of Climate**, v.19, p.3088-3111, 2006. DOI: <https://doi.org/10.1175/JCLI3790.1>.

STACKHOUSE JR., P.W. **POWER Data Methodology**. Version 1.0. 2020. Available at: <https://power.larc.nasa.gov/docs/methodology/>. Accessed on: Aug. 9 2023.

WHITE, J.W.; HOOGENBOOM, G.; STACKHOUSE JR., P.W.; HOELL, J.M. Evaluation of NASA satellite- and assimilation model-derived long-term daily temperature data over the continental US. **Agricultural and Forest Meteorology**, v.148, p.1574-1584, 2008. DOI: <https://doi.org/10.1016/j.agrformet.2008.05.017>.

ZAMBRANO-BIGIARINI, M. **hydroGOF**: goodness-of-fit functions for comparison of simulated and observed hydrological time series. R package version 0.4-0. 2020. DOI: <https://doi.org/10.5281/zenodo.839854>.